Journal of Solid State Chemistry **150,** 391–398 (2000)
doi:10.1006/jssc.1999.8612, available online at http://www.idealibrary.com on IDEAL®

Synthesis and Characterization of Diamine Intercalation Compounds of SnS_2 Single Crystals

Julián Morales,*,[1] Jesús Santos,* José R. Ramos Barrado,† Juán P. Espinós,‡ and Agustín R. González-Elipe‡

*Laboratorio de Química Inorgánica, Facultad de Ciencias, Universidad de Córdoba, Avda. S. Alberto Magno s/n, Córdoba, Spain; †Departamento de Física Aplicada, Facultad de Ciencias, Universidad de Málaga, Málaga, Spain; and ‡Instituto de Ciencias de Materiales, Centro Mixto Universidad de Sevilla-CSIC, P.O. Box 1115, Sevilla, Spain

Received October 14, 1999; in revised form November 30, 1999; accepted December 13, 1999

Single crystals of SnS_2 were intercalated with ethylenediamine (en) and propylenediamine (pn) by direct reaction. The resulting novel compounds were examined by different techniques including XRD, XPS, a.c. impedance, TG, and TPD measurements. The observed lattice expansion for both compounds, ca. 3.9 Å, is consistent with the location of the amine molecules at van der Waals gaps, with monolayers in the alkyl chain parallel to the sulfur layers. XPS data reveal that these complexes easily absorb moisture that binds strongly to sulfur to give hydrogen sulfide traces that were detected upon thermal deintercalation above 473 K. However, the charge transferred from the guest to the host is too small to be detected by this photoelectron technique. The en intercalate preserves the semiconductor behavior of the pristine compound, SnS_2, but with two significant differences, viz. lower conductivity at low temperatures and an increased activation energy. These differences are ascribed to increased incoherent scattering of electrons resulting from the guest atoms acting as impurities and also to the lattice defects formed upon intercalation.

Key Words: **aliphatic diamines; tin disulphide; intercalation.**

INTRODUCTION

One of the most salient properties of layered dichalcogenides is their ability to act as hosts for atomic and molecular guest species, which are accommodated at the empty sites bounded by van der Waals forces between adjacent close-packed chalcogen layers. This feature is of interest not only from a structural point of view but also by virtue of the changes in some physical properties—occasionally dramatic—involved. This has fostered extensive research since the earliest systematic studies on the topic carried out in the early 1970s. The information thus gathered was masterfully compiled in the now classic monograph by Whittingham and Jacobson (1). Many reviews and monographs have subsequently been published, the last, to our knowledge being that of Müller-Warmuth and Schöllhorn in 1994 (2). However, most of these studies have involved transition metal layered chalcogenides as hosts and a wide variety of guest species including both strong reductants, such as alkali metals, hydrazine, and organometallic compounds, and organic Lewis bases. By contrast, there are only a few studies on the intercalation properties of layered chalcogenides of nontransition elements. The prototypical family of these compounds is SnX_2 (X = S, Se), with CdI_2-related crystal structures. Their intercalation chemistry is indeed less extensively documented and only for SnX_2 intercalated with cobaltocene has an accurate description of the electronic properties been reported (3, 4). Alkali metal intercalation by chemical and electrochemical procedures has also been examined (5–7), essentially with the aim of elucidating structural details of the intercalation process. A different approach to the intercalation reaction that involves adsorption of the alkali metal onto single crystals in ultra-high vacuum, followed by examination of the electronic structure by photoelectron spectroscopy, has been proposed (8). Although this method avoids the presence of impurities, which may lead to spurious conclusions, some aspects of the process remain unresolved (particularly whether an intercalation or decomposition reaction occurs when the alkali metal atoms are deposited onto the clean surface of the crystals) (9).

The intercalation behavior of SnS_2 toward weaker electron donor guest molecules such as organic Lewis bases has so far rarely been studied in spite of the excellent structural flexibility of SnS_2, the lithiated phase of which can cointercalate organic molecules such as propylene carbonate and cause an expansion that exceeds the unit cell dimension by 12 Å (10). In continuing our research on the intercalation properties of SnS_2 single crystals, in this paper we report the preparation of novel intercalates with linear aliphatic

[1] To whom correspondence should be addressed. E-mail: iq1mopaj@uco.es.

0022-4596/00 $35.00

diamines and their characterization by using various analytical techniques. A complementary study of the electrical properties of the en intercalate was performed using a.c. impedance methods.

EXPERIMENTAL

The SnS_2 used was prepared as single crystals grown using a chemical transport method that started from a mixture of polycrystalline SnS_2 and I_2 (ca. 5 mg/cm^3) as carrier and sealed in an evacuated silica tube 20 cm long by 1.6 cm inner diameter. The tube was subjected to a temperature gradient of 923–823 K for one week and then allowed to gradually cool to room temperature. Under these conditions, golden plate-like crystals of variable size ranging from 1 to 5 mm in diameter and several tenths of a mm in thickness were obtained. The crystals were washed with acetonitrile to remove traces of I_2 and dried at 323 K prior to use as intercalation hosts. The amines used were reagent grade and supplied by Aldrich; they were further purified by distillation under argon and stored with a 0.3-nm molecular sieve supplied by Merck. About 200 mg of SnS_2 single crystals was sealed with 2 ml of *n*-alkyldiamine in a Pyrex tube and heated at 453 K. For en, 1 h was sufficient to obtain a pure intercalate; in contrast, pn required a longer period (18–24 h). Under these conditions, the crystals preserved their laminar morphology but the yellow color turned to black. The absence of X-ray reflections for the pristine compound, SnS_2, was taken to mark thorough intercalation. Products were filtered and washed with pure acetonitrile. All these manipulations were carried out in an MBraun dry glove box, where the intercalates were dried and stored.

The composition of the intercalates was determined by elemental analysis on a Fisons CNH instrument. Their thermal stability was examined by combining the results of a thermogravimetric analysis performed on a Cahn 2000 thermobalance under a dynamic argon atmosphere with those obtained from temperature programmed deintercalation (TPD) measurements made in a quartz reactor coupled to a quadrupole mass spectrometer (on Sensorlab model VG), using argon as the gas carrier.

Powder X-ray diffraction (XRD) patterns were recorded on a Siemens D-5000 diffractometer using graphite monochromatized Cu$K\alpha$ radiation and operating at 40 kV and 30 mA. For identification purposes, intensities were collected at 0.02 (2θ) intervals using 0.06 s per step. For the evaluation of the lattice parameters and broadening in the reflection lines, intensities were recorded in the same scan step at 3.6 s per step.

XPS spectra were recorded on an Scalab 210 spectrometer operating in the constant pass energy mode (50 eV) and using unmonochromatized Mg$K\alpha$ (1253.6 eV) radiation as the excitation source. Samples, made into pellets by compressing the crystals at about 3 tonnes under an argon atmosphere, were stuck onto a copper holder with the aid of a low vapor pressure epoxy resin and transferred to the spectrometer's preparation chamber. As all samples exhibited charging effects of 2–3 eV, the binding energy reference was taken at 161.6 eV for the S 2*p* core level, the value previously reported for S^{2-} in SnS_2 single crystals (9).

A.c. conductivity measurements were carried out on compact disks furnished with ionically blocking gold electrodes using a Solartron FRA 1255 frequency response analyzer and a Novocontrol BDC-N broadband dielectric converter; samples were placed in a Novocontrol holder the temperature of which was governed by a Quatro controller. The whole system was computer-controlled. The frequency range was 10 Hz to 3 MHz and the temperature range was 303–163 K. The compact disks, 13 mm in diameter and 1 mm thick, were prepared by pressing the crystals at 6 ton cm^{-2}.

RESULTS AND DISCUSSION

Aliphatic diamines, en and pn, can be readily intercalated into the host lattice SnS_2 by heating the organic liquid guest with the sulfide either in powder or single-crystal form under mild conditions. Large crystals of the intercalate single phases can be obtained with no mechanical stirring. Crystals from these samples were ground by hand and converted into powder of micrometer particle size range to evaluate their unit-cell dimensions from X-ray powder diffraction patterns (XRD) (see Fig. 1). The patterns for the pristine compound and the intercalates were indexed in the hexagonal system; the unit-cell constants obtained are given in Table 1. The calculated values for the host are quite consistent with previously reported data (11). Significantly, the *a* axis hardly changed upon treatment with the amine, which suggests little deformation in the layer plane. By contrast, a significant expansion along the *c* axis was observed, in good agreement with one of the main requirements for an intercalation reaction. Lattice expansion was similar for the two intercalates and reveals the little influence of the hydrocarbon chain length, which was previously observed in *n*-alkylamine complexes of TaS_2 and TiS_2 for carbon numbers up to 4 (12). The increase in the interlayer spacing is only slightly larger than the van der Waals diameter of the amine group (ca. 3.4 Å) and suggests that the diamine molecules form monolayers in the interlayer space with their longitudinal axis nearly parallel to the sulfur layers.

The amine intercalation process not only introduces changes in the positions of the diffraction peaks but also causes the originally rather sharp lines for the host to broaden significantly (see Fig. 1). This suggests a rupture of the coherent diffraction domains (crystallites) and/or an increase in the microstrain content of the host lattice upon

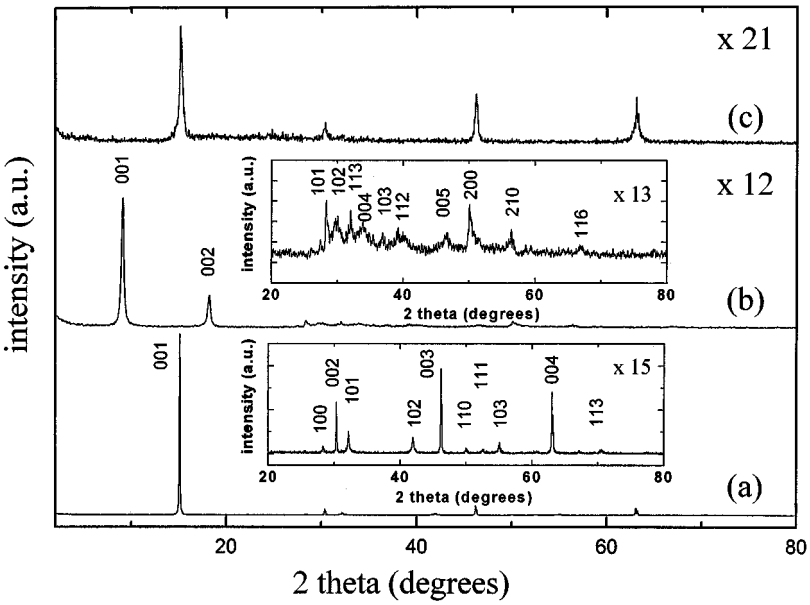

FIG. 1. XRD patterns for (a) SnS_2, (b) the SnS_2-en intercalate, and (c) the intercalate heated at 673 K. The factor indicates the magnification relative to curve *a*. The insets are enlarged by a factor relative to the whole pattern.

intercalation. These structural changes can be quantified by using multiple order (00l) lines and

$$(\delta 2\theta)^2 \cos^2\theta = 16\langle e^2\rangle \operatorname{sen}^2\theta + (k^2\lambda^2/L), \qquad [1]$$

which allows the separation of crystallite size and strain broadening (13). $\delta 2\theta$ is the integral breadth after correction for instrumental broadening from a highly crystalline silicon standard and $k\alpha_2$ elimination by the Rachinger method (14); $\langle e^2\rangle$ denotes local strains (defined as $\Delta d/d$, where d is the interplanar space); L is the crystallite size and k is a near-unity constant. Figure 2 shows selected plots of Eq. [1] for different reflections of the original and intercalated samples. Crystallite sizes and strains, calculated from the intercept and slope, respectively, are given in Table 2. As expected, the original compound exhibited a negligible intercept and slope, thus suggesting that the size of coherently diffraction domains, L, is large irrespective of the exfoliation properties of this material in the direction normal to [00l], and that the microstrain content, $\langle e^2\rangle$, is low, which is in good agreement with a highly crystalline powder. The amine treatment increased the microstrain content markedly (ca. 24 and 65 times for the en and pn intercalate, respectively), as reflected in an increased slope; in contrast, crystallite size decreased by a factor close to 6. Amine intercalation thus has two main effects, namely: (i) rupture of the coherent diffraction domain along the [00l] direction, which decreases the number of layers in each crystallite, and (ii) an increase in local strains probably due to the expansion required to accommodate the amine in the interlayer spacing.

The amine contents in the intercalates, obtained by C–N–H analysis, are shown in Table 1. The greatest differences between experimental and calculated values were those in the hydrogen content, and these were attributed to the presence of water that was probably picked up during handling of the intercalates in the air. The effect of the water is discussed below in describing thermal stability. The en complex was found to have an amine content higher than

TABLE 1
Structural and Analytical Data (in %) for SnS_2 and Diamine Complexes

Compound	a (Å)	c (Å)	Δd (Å)	C	N	H	P.D.
SnS_2	3.647 (1)	5.886 (3)	—	—	—	—	—
$SnS_2(en)_{0.37}$	3.649 (4)	9.780 (6)	3.90	4.28 (4.33)	5.00 (5.05)	1.57 (1.44)	1.1
$SnS_2(pn)_{0.45}$	3.645 (5)	9.713 (7)	3.83	7.40 (7.50)	5.63 (5.83)	2.20 (2.08)	1.6

Note. Calculated values are given in brackets.

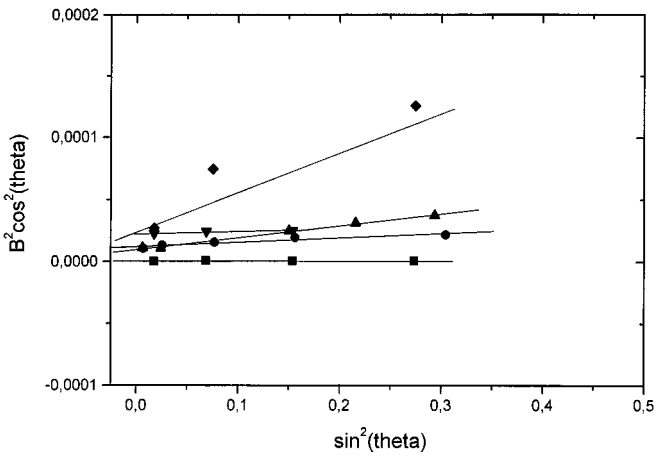

FIG. 2. Plots of Eq. [1] for different (00l) reflections. Pristine SnS_2 (■); SnS_2-en intercalate at room temperature (●) and heated at 673 K (▼); SnS_2-pn intercalate at room temperature (▲) and heated at 673 (◆).

those of 1T–TaS_2 (15) and 6*R*–TaS_2 (16), the stoichiometry of which was $TaS_2(en)_{1/4}$, and somewhat greater than that reported for TiS_2, $TiS_2(en)_{0.29}$ (17). However, we could not obtain a pure TiS_2-en complex under conditions similar to those for the SnS_2-en system (18).

The packing density of the amine intercalates (PD) was determined by combining the amine content with the cross-sectional area of the amine molecule (1) and the area of the basal plane of SnS_2. The results obtained are shown in Table 1. PD for the en complex was close to the unity, so the amine molecules are highly packed and occupy all empty sites in the interlayer space. However, PD for the pn complex clearly exceeds unity. In addition to those at van der Waals sites, molecules must therefore exist bound to the surface as shown below.

Intercalate stability was examined by combining the thermogravimetric data obtained under a dynamic argon atmosphere with those of the analysis of evolved gases by mass spectrometry. The temperature range studied was 298–673 K. Amine release monitored in the mass spectrum was via the *m*/*z* 30 fragment; the base peak for H_2S was also recorded as this compound is usually encountered in thermal deintercalation studies of layer chalcogenides intercalated with organic molecules (18, 19). Figure 3 shows the TG and TPD curves for the two intercalates. For both compounds, the total weight loss exceeded to the amine content calculated by elemental analysis. A similar behavior was also previously observed in TaS_2-en complexes (15); although the amine content was determined by a standard weight gain method, the explanation proposed (a high binding energy leading to destructive deintercalation) seems unlikely in light of our results. However, significant differences are observed in the profiles of the thermal curves. Thus, the pn complex exhibits weight losses in at least two successive stages, centered at 393 and 548 K, both involving the release of amine molecules (see Fig. 3); this suggests the presence of more than one type of amine species bound to the host. On the assumption that the weight loss recorded between ca. 423 and 623 K corresponded to the intercalated amine, a SnS_2 $(pn)_{0.35}$ stoichiometry was obtained; however, the amine content must be somewhat smaller as the weight loss also includes released H_2S and possibly some H_2O that could not be confirmed due to the background of H_2O in the spectrometer. In fact, the packing density resulting from this stoichiometry was 1.2, which is slightly greater than unity.

Based on the XRD pattern recorded after thermal treatment of the sample at 448 K, (between the first and second stage), the intercalate structure was preserved. This strongly

TABLE 2
Crystallite Size and Microstrains for Pristine and Diamine Intercalates

Compound	*L* (Å)	$\langle e^2 \rangle \times 10^6$
SnS_2	2851	0.092
$SnS_2(en)_{0.37}$	440	2.2
$SnS_2(pn)_{0.45}$	487	6.0
en complex (400°C)	324	1.2
pn complex (400°C)	278	22

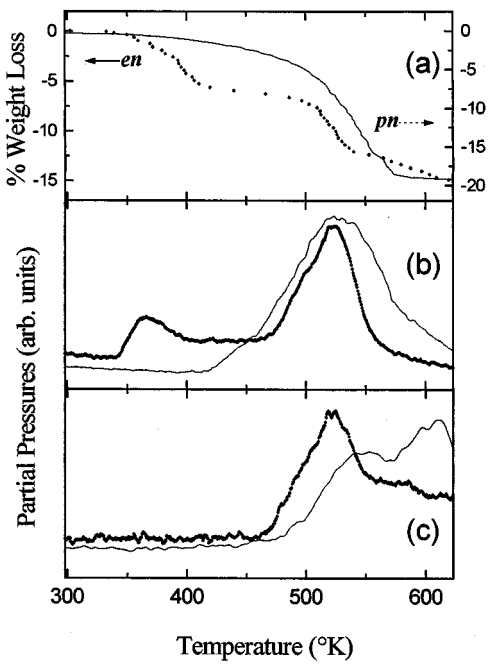

FIG. 3. Thermal deintercalation data for SnS_2-en (—) and SnS_2-pn (●●●) intercalates. (a) Thermogravimetric curves; (b) temperature programmed deintercalation spectra for the amine (*m*/*z* 30) and (c) H_2S (*m*/*z* 34) base peaks.

supports the assumption that pn evolved around 398 K does not reside in the interlayer spacing but rather binds to the surface and must be the origin of the high content measured by elemental analysis, in comparison with that obtained for the en intercalate. In contrast, the TG curve for the en complex exhibits basically a single weight loss, in good agreement with the amine profile of the TPD spectrum; this exhibits a single and rather symmetric peak centered at ca. 528 K suggestive of the presence of a single type of amine in the interlayer positions. On the other hand, the high temperature of the peak for the pn complex (548 K), relative to the en compound (528 K) is somewhat uncommon and may lead one to spuriously assign a greater stability to the former complex. In fact, for both compounds, the amine is released largely over the 473–573 K range, so it is difficult to distinguish the two systems in terms of thermal stability.

Also of interest is the formation of H_2S as the amine molecules at van der Waals gaps are released. At least two models could account for its formation, viz. direct attack by water molecules,

$$H_2O + S^{2-}\ (\text{lattice}) \rightarrow H_2S + O^{2-}\ (\text{lattice}), \qquad [2]$$

or via the intercalation mechanism proposed by Schöllhorn *et al.* (20), which is based on a protonation process during which a certain fraction of the intercalant amine groups is provided with an extra proton that can be shared with neighboring unprotonated guest molecules. This proton could be transferred to sulfur atoms of the host, thus promoting the formation of H_2S and the subsequent formation of vacancies.

The binding energies of the main core levels for SnS_2 and $SnS_2(en)_{0.37}$ are given in Table 3. The emission peaks of Sn (3*d*), S (2*p*), and N (1*s*) are shown in Fig. 4. Oxygen-containing compounds were detected in the intercalates by XPS (at least at particle surface). Part of this oxygen was strongly bound to sulfur, as suggested by the higher binding energy component found in the S 2*p* photoemission peak (see Table 3 and Fig. 4a). In contrast, the Sn peaks maintained a high symmetry and no new peaks assigned to this element were detected in spite of the structural deterioration undergone by the host (Fig. 4b). However, the binding energies increased of about 0.4 eV, thus approaching to that for SnO_2 (487.5 eV) (21). A more pronounced difference was found in the modified Auger parameter (defined as the sum of the binding energy of the photoelectron and the kinetic energy of the corresponding Auger transition) for Sn. This parameter is free from calibration errors and is more sensitive to chemical state than are chemical shifts (22). The modified Auger parameter calculated for the Sn $3d_{5/2}$ emission peak and the Sn_{MNN} Auger electron transition shifted from 920.8 (SnS_2) to 918.9 eV [$SnS_2(en)_{0.37}$]. This latter value is still closer to that of SnO_2 (918.5 eV) (21). These results reveal that the local environment of Sn atoms is affected by the oxygen content and suggest that the amine intercalation increases the reactivity of the host toward water, which is responsible for the surface deterioration of crystals. This water must be the origin of the discrepancy between the results of the elemental analysis and weight loss measurements. The difference in the analysis by the two methodologies was similar for both intercalates (approximately 3%); an accurate estimate of the water content could not be obtained because the amount of H_2S was unknown at the time. The spectroscopic data also support the model of Eq. [2] for the release of H_2S. In any case, the release of H_2S and the amine extrusion do not completely collapse the host lattice even though they induce a significant degradation (to the extent that little crystalline material remains). The only phase present in the heat-treated intercalates was found to be SnS_2, the XRD pattern of which exhibited a significant decrease in intensity and increased broadening in the diffraction lines (see Fig. 1c). Other possible phases formed in accordance with Eq. [2] such as SnO_2 were not detected by XRD, either because the amount of sulfur released was too low and/or because the oxygen-containing phase was amorphous. In contrast, the lattice preserves the strong distortion caused by the amine intercalation, which tends to increase rupture in the diffraction domains along the [00l] direction (see Table 2).

One other interesting finding in the XPS spectra was the asymmetry in the N 1*s* profile shown in Fig. 4c, previously reported for other en chalcogenide complexes (18); its origin has been associated to the presence of two types of organic molecules bound to the chalcogen layers. The peak can be resolved in two components centered at 400.1 and 400.9 eV, which are somewhat greater than the reported values for free diamines (398.8 eV) (23). The profile asymmetry is consistent with the XPS spectra for NbS_2 and TaS_2 intercalated with simple nitrogenous bases (24, 25). Moreover, in these intercalates the N 1*s* line also appears to a binding energy greater than that of pure amines. This shift has been attributed to a decrease in the electron density at the nitrogen, thus involving a donation of charge from the nitrogen to the TS_2 layers. However, the differences between the valence band spectra for SnS_2 and $SnS_2(en)_{0.37}$ near to the Fermi

TABLE 3
Binding Energies (in eV) of the Main Core Level Spectrum for the SnS_2-en Complex

Compound	S 2*p*	Sn $3d_{5/2}$	Sn 4*d*	N 1*s*	C 1*s*	O 1*s*
SnS_2	161.6	486.5	25.8	—	—	—
$SnS_2(en)_{0.37}$	161.6	486.9	26.2	400.1	285.8	531.5
	168.3			400.9		

Note. The values for SnS_2 are included for comparison.

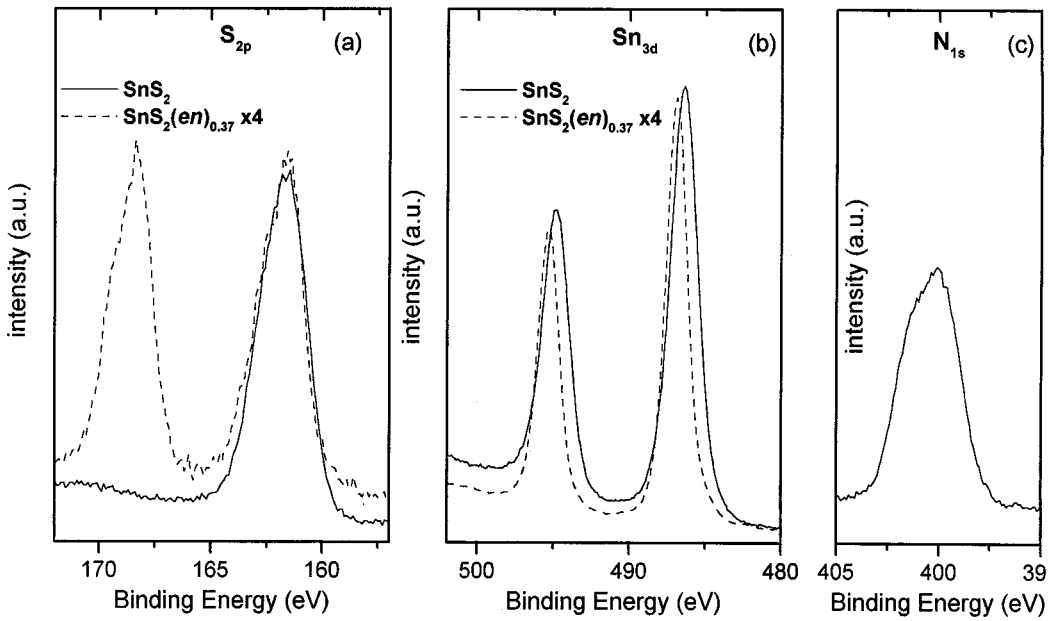

FIG. 4. S 2*p*, Sn 3*d*, and N 1*s* core-level spectra for SnS_2 and SnS_2-en intercalate. The factor indicates the magnification relative to the spectrum of pristine compound.

region, shown in Fig. 5, are insignificant. The different peaks of the SnS_2 XPS spectrum can be assigned to the bands formed by the overlap of Sn (5*s*, 5*p*) and S (3*s*, 3*p*) orbitals (26). A closer inspection to the difference spectrum, Fig. 5c, reveals that the electron density at the Fermi level barely changes, in contrast to that observed in the SnS_2–$CoCp_2$ system studied by ultraviolet electron spectroscopy (4) that shows a small peak near to the Fermi level upon intercalation. These additional states have been ascribed to the electrons transferred from the guest to the host. The negative values in the difference spectrum, that appear as a peak centered at ca. 2.5 eV, were also found in SnS_2 intercalated with cobaltocene (4), and their origin is a consequence of the significant reduction observed for the emission at ca. 2.5 eV

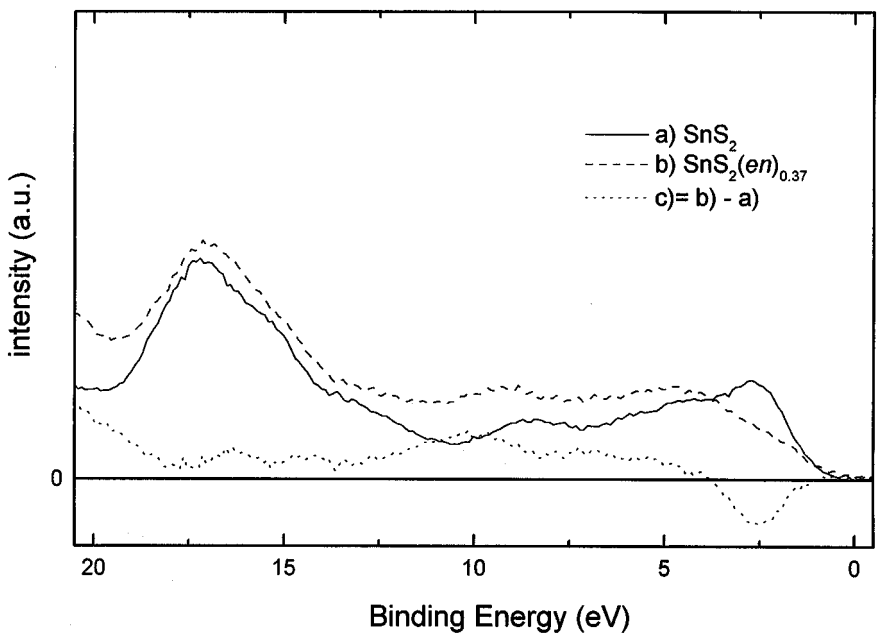

FIG. 5. Valence band region of the XPS spectra for (a) SnS_2, (b) SnS_2-en intercalate, and (c) difference spectrum.

relative to the intensity of the peak at ca. 17.2 eV. At present, we lack a suitable explanation for this unusual behavior. The weak and broad emission peak in the ca. 8–13 eV binding energy range could be assigned to O 2*p* states. Thus, these results indicate that experimental evidence of the charge transferred from the organic molecule to the empty band of the disulfide is limited, probably because the charge transfer must be too small to be detected by XPS (partly owing to the lack of resolution of the X-ray source used to study the valence band).

Figure 6 shows the Nyquist plots of complex impedance for SnS_2 and $SnS_2(en)_{0.37}$ recorded at 303 K. Experimental data were fitted using a nonlinear least-squares (NLLS) method (27) that allows the a.c. impedance of a physical system to be modeled by an electrical circuit which is included in Fig. 6 and composed by a serial association of two subcircuits made up of a parallel association of a resistance and a constant phase element. Both subcircuits (*RQ*, where *Q* is a constant phase element) represent processes between grain boundaries (gb) and into the bulk (b). Figure 7 shows the the temperature variation of the d.c. bulk conductivity obtained from equivalent circuits. These results reveal an increase in conductivity with increasing temperature for both samples that suggests a semiconductor behavior throughout the temperature range studied. In fact, SnS_2 is an *n*-type semiconductor with a band gap energy of 2.17 eV (28). These data warrant several comments. Below 275 K, a decrease in conductivity upon intercalation is observed. Above 275 K, the conductivity of the intercalate reaches and surpasses that of SnS_2. These results are in contrast with those for in SnS_2 treated with cobaltocene, the conductivity of which was found to significantly increase on intercalation throughout the temperature range studied (180–300 K) (3). However, there is a remarkable similarity with those reported for $NbSe_2$ intercalated with en (15). In this case, and although both systems exhibit a metallic behavior, a decrease in conductivity was measured upon

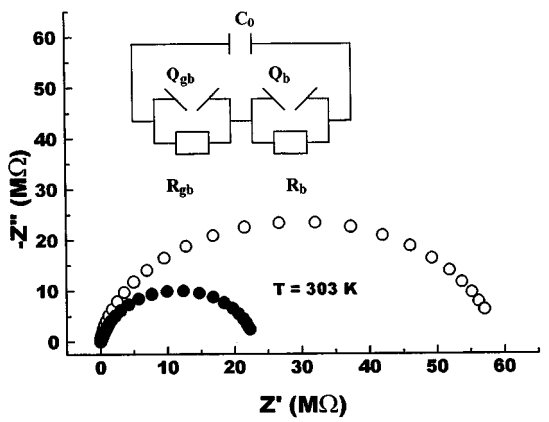

FIG. 6. Nyquist plots for (○) SnS_2 and (●) the SnS_2-en intercalate. The inset shows the equivalent circuit to model the data.

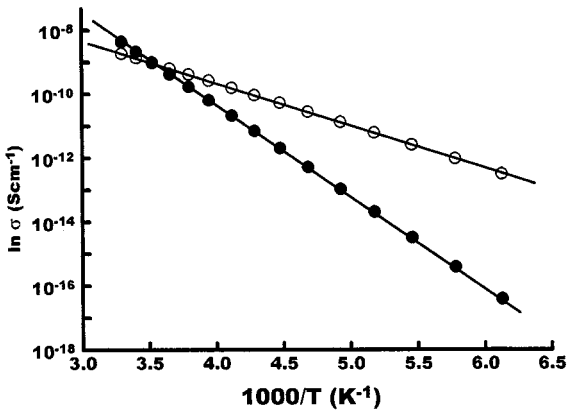

FIG. 7. Arrhenius plots for (○) SnS_2 and ●) the SnS_2-en intercalate.

intercalation the origin of which was explained in the light of the model of tunneling through a barrier. Besides, the slopes of the temperature dependence plots are similar to those of Fig. 7 and the conductivity of the intercalate must exceed that of the pristine compound above 273 K (the highest temperature reported). A conductivity decrease was also previously observed in 4H–TaS_2 intercalated with en (15).

Plots of $\ln \sigma$ vs $1/T$ were found to be linear and provided an activation energy of 0.18 and 0.47 eV for pristine SnS_2 and the en complex, respectively. The calculated value for unintercalated SnS_2 was similar to that obtained by O'Hare *et al.* (3) for single crystals using a d.c. four-probe method. However, the activation energy of cobaltocene intercalate, $SnS_2\{CoCp_2\}_{0.30}$, was similar to that of SnS_2 although its conductivity was more than 200 times higher than that of the unreacted host. This behavior is ascribed to changes in the electronic structure of both the host and the guest upon intercalation. Transferred electrons from cobaltocene, a strong reductant, and its subsequent oxidation to cobalticinium ion, $CoCp_2^+$, give an impurity band close to the conduction band of the semiconductor. Chemically, these electrons are transferred to the empty Sn 5*s* state and lead to the formation of an Sn(II) valency. However, this model is unsuitable for the SnS_2-en system for the following reasons: (i) the driving force for intercalation here is not a redox process (rather, bonding between the intercalant and the host is better described as a weak covalent interaction between the nitrogen lone pair and antibonding or nonbonding empty cation sites) (12); (ii) XPS is unable to detect two oxidation states for tin and significant shifts in the valence band spectrum of SnS_2 treated with en.

One alternative model that can be used to justify the conductivity data of Fig. 7, the homosolvation mechanism suggested by Schöllhorn *et al.* (20), which is based on an ionic model, is also difficult to apply to the SnS_2-en system. In our case, the intercalate stoichiometry should have been

$[SnS_2]^{x-}(enH^+)_x(en)_y$ and the source of protons could have been impurities such as water. Thus, the conductivity could be the result of both electronic and ionic contributions. However, conductivity data would have exhibited a nonlinear behavior unlike that reflected in Fig. 7. Moreover, the a.c. impedance data lead to typical semicircular plots (see Fig. 6) and the lack of electrode polarization in the low frequency region suggests that the charge is not blocked at the electrode interface, so the current is carried largely by electrons.

The decreased conductivity of the intercalate at low temperatures must primarily be due to incoherent scattering of the electrons by impurity atoms—the guest molecules—and the lattice defects arising from intercalation. On the other hand, its greater activation energy is partially offset by an increased preexponential factor, whose conductivity dependence is $E_a\sigma$. This type of behavior is known as the Meyer–Nedel compensation rule (29). One common qualitative argument in favor of this rule is the increased activation entropy in cases where the escape over a high barrier requires a multistep process.

CONCLUSIONS

In summary, we have shown that SnS_2 single crystals readily undergo a direct reaction with aliphatic diamines, (en, pn), to form new intercalation compounds that preserve the hexagonal symmetry of the host and exhibit a *c*-axis expansion of ca. 3.9 Å, which is comparable to the van der Waals diameter of the amine groups. The complexes are quite stable and deintercalation takes place at temperatures above 473 K, with simultaneous formation of H_2S (probably through direct attack of water on the lattice as they absorb moisture under ambient conditions). The conductivity of the en complex exhibits a temperature dependence of the Arrhenius type with an activation energy nearly three times greater than that of unintercalated SnS_2. Below 274 K, the intercalate conductivity is also lower than that of SnS_2, probably as a result of a decreased mobility of the current carriers due to the presence of insulating organic molecules and to the strong distortion in the lattice.

ACKNOWLEDGMENTS

The authors gratefully acknowledge support from CICyT (Project PB95-0561) and Junta de Andalucía (Groups FQM 175 and 192).

REFERENCES

1. M. S. Whittingham and A. J. Jacobson (Eds.), "Intercalation Chemistry." Academic Press, New York, 1982.
2. W. Müller-Warmuth and R. Schöllhorn (Eds.), "Progress in Intercalation Research." Kluwer, Dordrecht, 1994.
3. D. O'Hare, W. Jaegermann, D. L. Williamson, F. S. Ohuchi, and B. A. Parkinson, *Inorg. Chem.* **27,** 1537 (1988).
4. C. A. Formstone, E. T. FitzGerald, P. A. Cox, and D. O'Hare, *Inorg. Chem.* **29,** 3860 (1990).
5. M. Danot, A. le Blanc, and J. Rouxel, *Bull. Soc. Chim. Fr.* **8,** 2670 (1969).
6. R. Schöllhorn, W. Roer, and K. Wagner, *Monat. Chemie* **110,** 1147 (1972).
7. J. Morales, C. Pérez Vicente, J. Santos, and J. L. Tirado, *Electrochim. Acta* **42,** 357 (1997).
8. M. Bronald, C. Pettenkofer, and W. Jaegermann, *Appl. Phys. A* **52,** 171 (1991).
9. J. P. Espinós, A. R. González Elipe, L. Hernán, J. Morales, J. Santos, and L. Sánchez, *Surf. Sci.* **426,** 259 (1999).
10. L. Hernán, J. Morales, J. Santos, and L. Sánchez, *J. Electrochem. Soc.* **146,** 657 (1999).
11. A. K. Grarg, *J. Phys. C*: *Solid Sate Phys.* **19,** 3949 (1986).
12. F. R. Gamble, J. H. Osiecki, M. Cais, R. Pisharrody, F. J. Disalvo, and T. H. Geballe, *Science* **174,** 493 (1971).
13. H. P. Klug and L. E. Alexander "X-ray Diffraction Procedures for Polycrystalline and Amorphous Materials." Willey, New York, 1974.
14. W. A. Rachinger, *J. Sci. Instrum.* **25,** 254 (1948).
15. S. F. Meyer, R. E. Howard, G. R. Stewart, J. V. Acrivos, and T. H. Geballe, *J. Chem. Phys.* **62**, 4411 (1975).
16. E. Figueroa, J. W. Brill, and J. P. Selegue, *J. Phys. Chem. Solids* **57,** 1123 (1996).
17. H. Ogata, H. Fujimori, S. Miyajima, K. Kobashi, T. Chiba, R. E. Taylor, and K. Endo, *J. Phys. Chem. Solids* **58,** 701 (1997).
18. L. Hernán, J. Morales, J. Santos, J. P. Espinós, and A. R. González Elipe, *J. Mater. Chem.* **8,** 2281 (1998).
19. P. A. Joy and S. Vasudevan, *Chem. Mater.* **5,** 1182 (1993).
20. R. Schöllhorn and H. D. Zayefka, *Angew. Chem. Int. Ed. Engl.* **16,** 199 (1977).
21. V. M. Jiménez, J. A. Mejías, J. P. Espinós, and A. R. González Elipe, *Surf. Sci.* **366,** (1996) 545.
22. C. D. Wagner, *Faraday Discuss. Chem. Soc.* **60,** 291 (1975).
23. F. Parmigiom and L. E. Depero, *Struct. Chem.* **5,** 117 (1993).
24. B. Bach and J. M. Thomas, *J. Chem. Soc. Chem. Commun.* 302 (1972).
25. F. R. Gamble, J. M. Osiecki, and F. J. DiSalvo, *J. Chem. Phys.* **55,** 3525 (1971).
26. F. R. Shepherd and P. M. Williams, *J. Phys. C* **7,** 4416 (1974).
27. B. A. Boukamp, *Solid State Ionics* **20,** 31 (1986).
28. T. Shibata, N. Kambe, Y. Muranushi, T. Miura, and T. Kishi, *J. Phys. D*: *Appl. Phys.* **23,** 719 (1990).
29. W Meyer and H. Nedel, *Z. Tech. Phys.* **12,** 158 (1937).